Liquid-Rocket Transverse Triggered Combustion Instability: Deterministic and Stochastic Analyses

by W. A. Sirignano
Mechanical and Aerospace Engineering
University of California, Irvine

Collaborators: P. P. Popov and A. Sideris

Support: Air Force Office of Scientific Research
Dr. Mitat Birkan, Program Manager

Modes of Transverse Oscillation

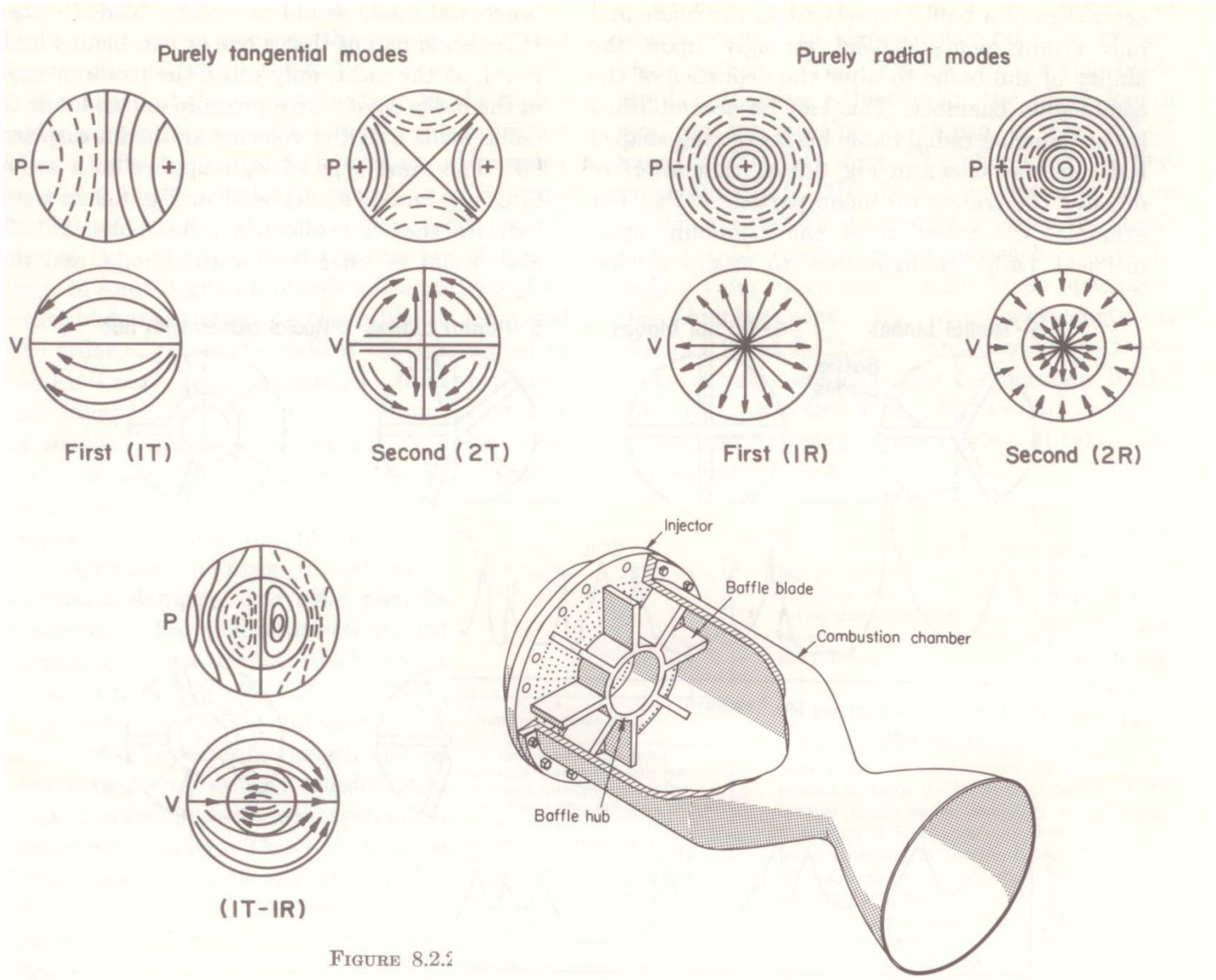

FIGURE 8.2.2

Nonlinear Combustion Instability and Triggering Action

Princeton experiment, circa 1961. A "bomb" (gunpowder contained with burst disk) is used as the trigger.

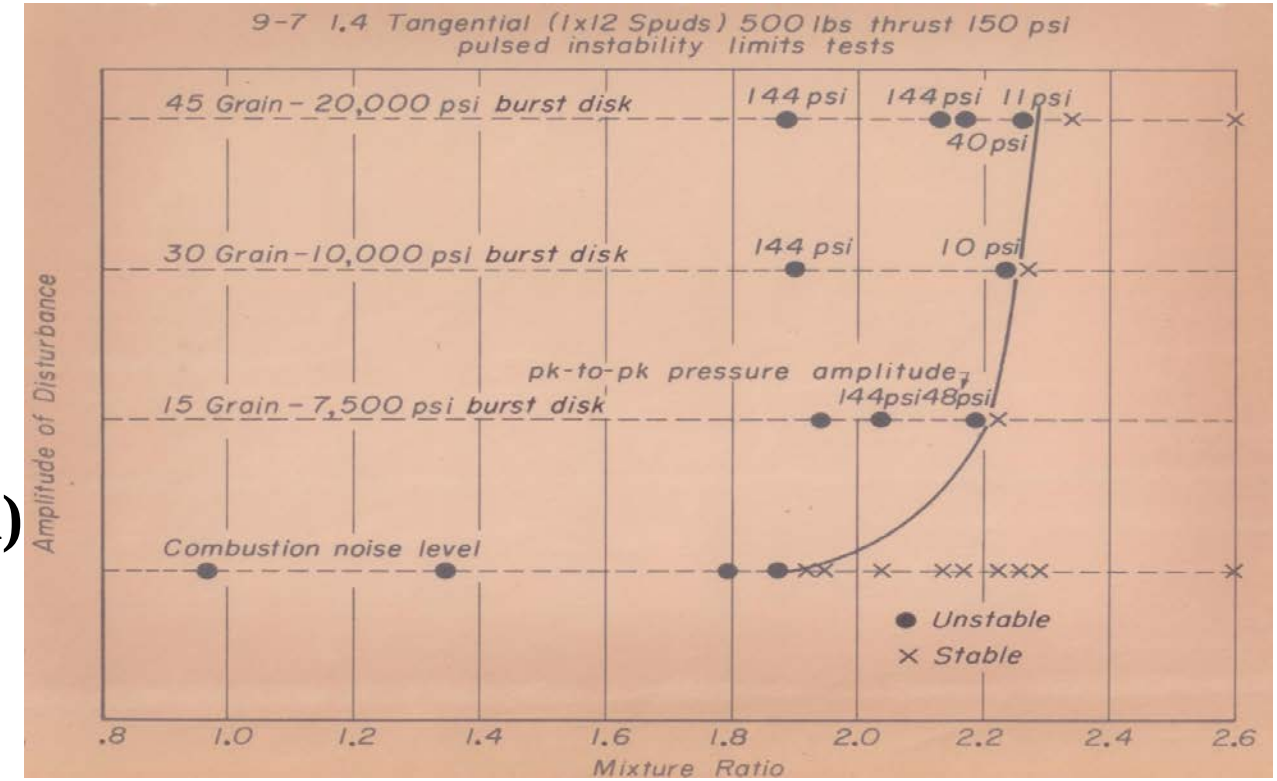

Instability initiates in various ways, depending upon the operational domain: (1) oscillations growing from combustion noise are named linear or spontaneous instabilities; (2) oscillations initiated only by disturbances larger than noise are named nonlinear or triggered instabilities. All limit-cycle oscillations are nonlinear; "linear" and "nonlinear" refer to initiation.

EARLY THEORIES

Nonlinear limit cycles were first predicted by Crocco & students in the 1960s using perturbation methods: Sirignano, Zinn, and Mitchell dissertations. Triggering and stable and unstable limit cycles were predicted.

Later, Zinn & Powell followed by Culick and co-workers used a Galerkin method to predict transient behavior as well.

Except for one portion of Sirignano's work, all the models used heuristic representations of combustion: e.g., n, τ model.

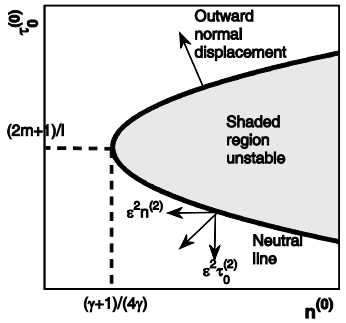

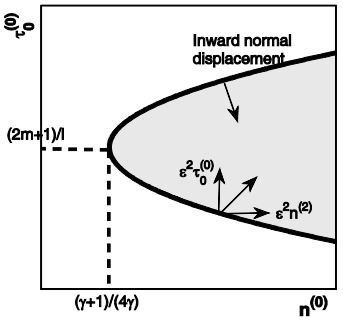

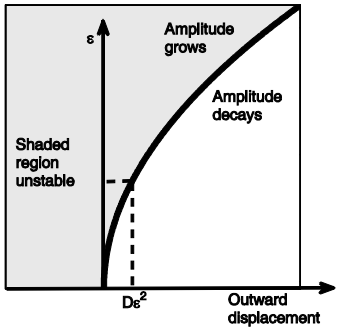

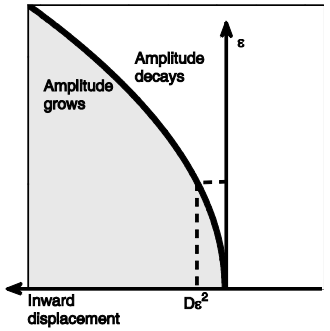

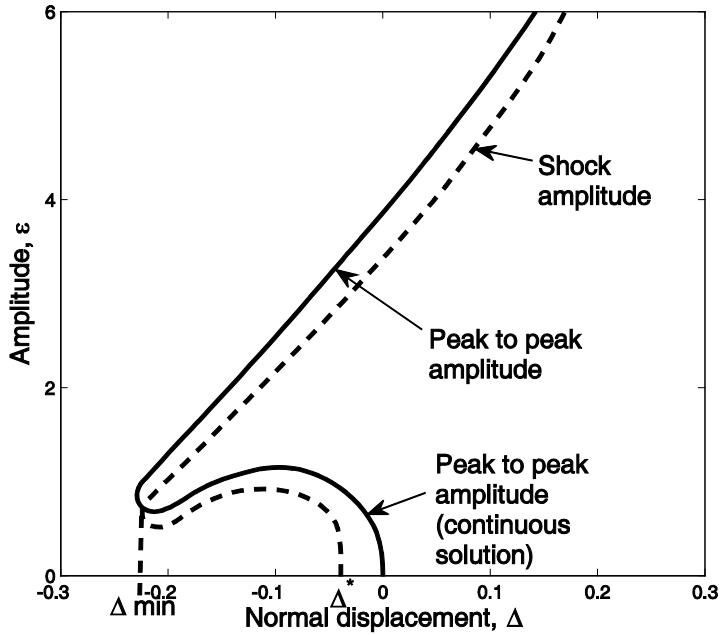

Goals of Current UCI Combustion Instability Research

- **Develop “simplified” liquid-rocket numerical model of combustion dynamics to test stochastic approaches and demonstrate the triggering of combustion instabilities.**
- **Examine nonlinear stability. Identify parameter domains allowing triggering.**
- **Determine whether different pressure and velocity disturbance profiles lead to different limit cycles.**
- **Extend the model with the inclusion of stochastic terms representing large-amplitude random perturbations. Perform the uncertainty quantification analysis.**
- ***Future:*** **Extend the work to more detailed combustion dynamics models in collaboration with Georgia Tech and HyPerComp.**

Model Equation System

- **The model equations retain essential combustion dynamics but eliminate much of the secondary physics which could be added in later studies. This model should allow the testing of our statistical approaches before we engage in a full analysis.**
- **The focus is on transverse oscillations in a cylindrical chamber allowing averaging over the axial direction and reduction to an unsteady, two-dimensional problem in the transverse polar coordinates.**
- **Kinematic waves are neglected leaving only the longer acoustic waves. These kinematic waves travel primarily in the axial direction and because of larger gradients (i.e., shorter wavelengths) are more likely to be vitiated by turbulent mixing.**
- **Viscosity, heat-conductive, and turbulent-mixing effects on the longer acoustic waves are neglected.**
- **A model for co-axial stream turbulent mixing and reaction is developed and employed for a multi-injector configuration.**
- **A simplified “short” multi-orifice nozzle boundary condition is used. Entrance Mach number remains constant.**

Nonlinear Wave Equation for Pressure

$$\frac{\partial^2 p}{\partial t^2} + Ap^{\frac{\gamma-1}{2\gamma}}\frac{\partial p}{\partial t} - Bp^{\frac{\gamma-1}{\gamma}}\left[\frac{\partial^2 p}{\partial r^2} + \frac{1}{r}\frac{\partial p}{\partial r} + \frac{1}{r^2}\frac{\partial^2 p}{\partial \theta^2}\right] = \frac{(\gamma-1)}{\gamma}\frac{1}{p}\left(\frac{\partial p}{\partial t}\right)^2 + (\gamma-1)\frac{\partial E}{\partial t}$$

$$+\gamma p^{\frac{\gamma-1}{\gamma}}\left[\frac{\partial^2 (p^{\frac{1}{\gamma}}u_r^2)}{\partial r^2} + \frac{2}{r}\frac{\partial (p^{\frac{1}{\gamma}}u_r^2)}{\partial r}\right.$$

$$+\frac{2}{r}\frac{\partial^2 (p^{\frac{1}{\gamma}}u_r u_\theta)}{\partial r \partial \theta} + +\frac{2}{r^2}\frac{\partial (p^{\frac{1}{\gamma}}u_r u_\theta)}{\partial \theta}$$

$$\left.+\frac{1}{r^2}\frac{\partial^2 (p^{\frac{1}{\gamma}}u_\theta^2)}{\partial \theta^2} - \frac{1}{r}\frac{\partial (p^{\frac{1}{\gamma}}u_\theta^2)}{\partial r}\right]$$

E **is the energy per unit volume per unit time released by the combustion process. Modelling of** ***E*** **is required.**

Momentum equations for radial and azimuthal velocities

$$\frac{\partial u_r}{\partial t} + u_r\frac{\partial u_r}{\partial r} + u_\theta\frac{1}{r}\frac{\partial u_r}{\partial \theta} - \frac{u_\theta^2}{r} + \frac{C}{p^{\frac{1}{\gamma}}}\frac{\partial p}{\partial r} = 0 \qquad \frac{\partial u_\theta}{\partial t} + u_r\frac{\partial u_\theta}{\partial r} + u_\theta\frac{1}{r}\frac{\partial u_\theta}{\partial \theta} + \frac{u_r u_\theta}{r} + \frac{C}{rp^{\frac{1}{\gamma}}}\frac{\partial p}{\partial \theta} = 0$$

Triggering disturbance could appear in several ways:

-- Introduction through reacting, mixing flow-field condition

-- Introduction through injector-face boundary condition.

-- An intermittent blockage in nozzle flow.

CONFIGURATION: Ten oxygen-methane co-axial injectors are placed in a combustion chamber. The model equation is solved with a co-axial mixing and reaction for the heat-release.

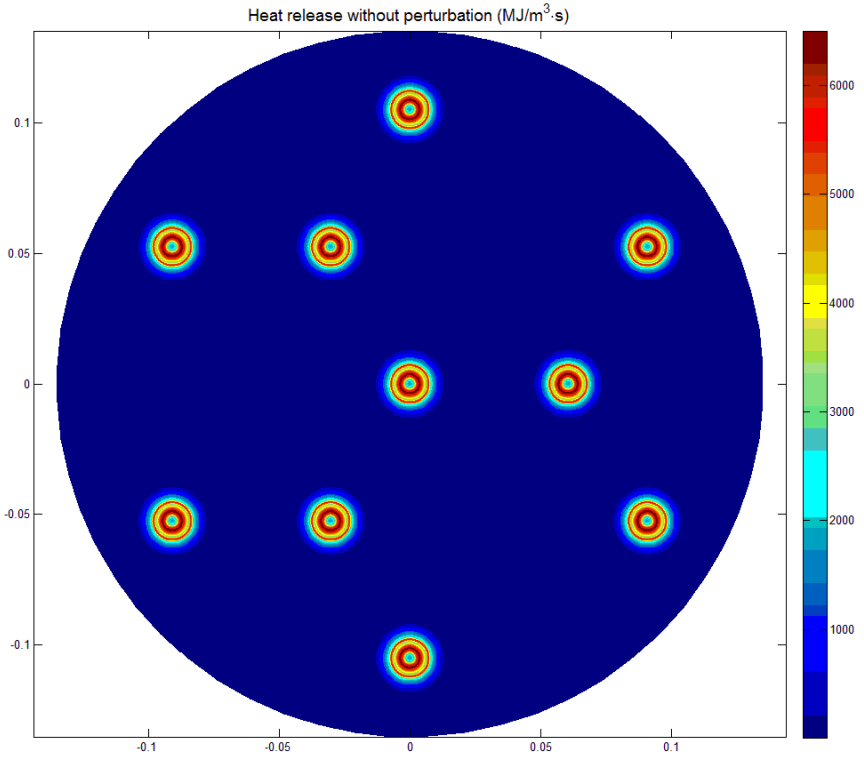

- **Chamber length is 0.5m and diameter is 0.28m .**
- **Injector outer diameter, 1.1cm**
- **Injector inner wall 0.898 cm**
- **Inner flow of gaseous oxygen,**
- **Outer flow of methane gas**
- **“Short” multi-orifice nozzle**
- **Steady-state pressure is 200atm, temperature is 2000K**

First, an individual injector is examined subject to a prescribed pressure oscillation; then, the analysis is made with ten injectors coupled to the chamber wave dynamics.

Co-axial Mixing Model
Energy and Species Equations

minus

$$\rho\frac{\partial h}{\partial t}+\rho\vec{u}\cdot\nabla h+k\nabla^2 T-\frac{\partial p}{\partial t}-\vec{u}\cdot\nabla p=\rho\dot{Q}=\rho Q\omega_F$$

$$\kappa=T-T_o(p/p_o)^{(\gamma-1)/\gamma}$$

$$\frac{\partial \kappa}{\partial t}+\vec{u}\cdot\nabla\kappa+D\nabla^2\kappa=\frac{Q}{c_p}\omega_F$$

minus

$$\frac{\partial Y_i}{\partial t}+\vec{u}\cdot\nabla Y_i+D\nabla^2 Y_i=\omega_i$$

minus

Uniform pressure over jet
One-step reaction
Le = 1
Use eddy diffusivity for *D*

$$D=\frac{U(t)R_o}{24.5},$$

Ambient gas oscillates isentropically.
P and T are collapsed to one function of entropy.

Schvab-Zel'dovich Variables

$$\alpha = Y_F - \nu Y_O - Y_{F,o}$$

$$\frac{\partial \alpha}{\partial t} + \vec{u} \cdot \nabla \alpha - D\nabla^2 \alpha = 0$$

$$\beta = \kappa - (Q/c_p)(Y_F - Y_{F,o})$$

$$\frac{\partial \beta}{\partial t} + \vec{u} \cdot \nabla \beta - D\nabla^2 \beta = 0$$

$$\frac{\partial \alpha}{\partial t} + U(t)\frac{\partial \alpha}{\partial x} - D\left[\frac{\partial^2 \alpha}{\partial r^2} + \frac{1}{r}\frac{\partial \alpha}{\partial r}\right] = 0$$

$$\frac{\partial \beta}{\partial t} + U(t)\frac{\partial \beta}{\partial x} - D\left[\frac{\partial^2 \beta}{\partial r^2} + \frac{1}{r}\frac{\partial \beta}{\partial r}\right] = 0$$

$$\frac{\partial Y_F}{\partial t} + U(t)\frac{\partial Y_F}{\partial x} - D\left[\frac{\partial^2 Y_F}{\partial r^2} + \frac{1}{r}\frac{\partial Y_F}{\partial r}\right] = \omega_F$$

S-Z formulation plus Oseen approximation reduces three nonlinear PDEs to one nonlinear PDE and two linear, homogeneous PDEs. We may use Green's function for two equations or numerical integration for all three equations.

Peer Review

A multi-scale problem is treated with a large-scale computational grid for the chamber wave dynamics and N fine grids for the jet flames at the N co-axial injectors.

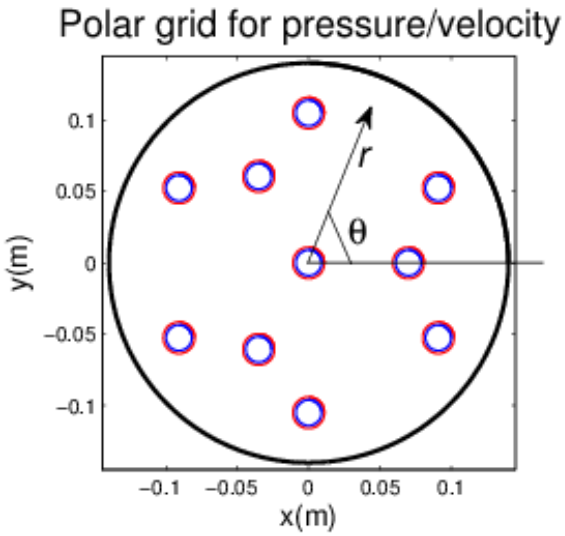

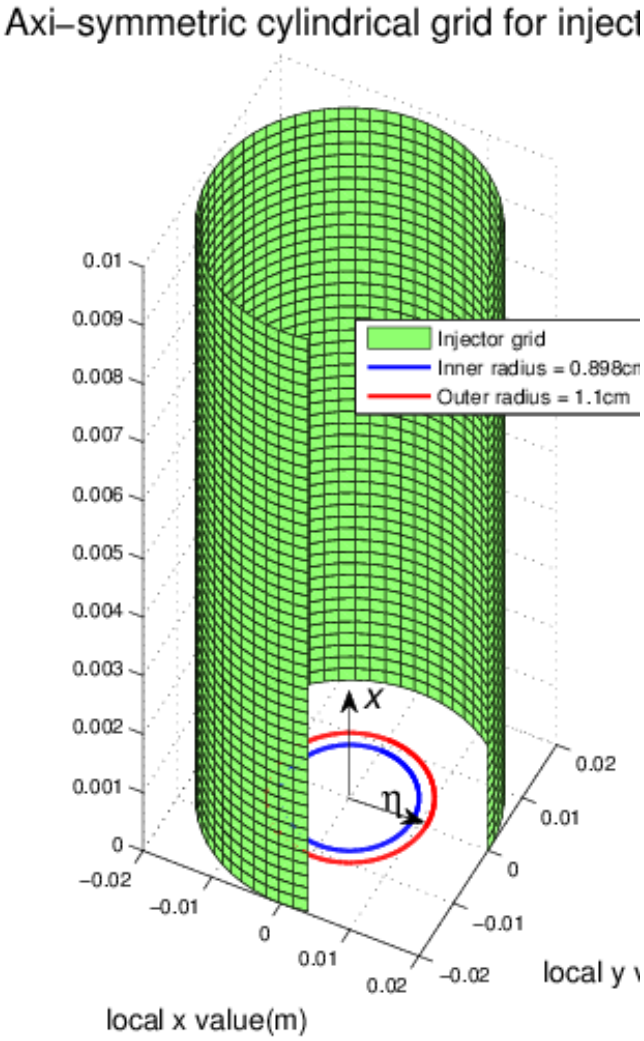

Frequency Response of Single Injector

- Sinusoidal pressure of frequency f.
- Two characteristic combustion times appear: τ_M for turbulent mixing, τ_R for chemical reaction.
- Time-lag: energy release rate E lags the pressure p oscillation.
- Reaction rate pre-exponental factor is varied from known value to explore frequency response for two time ratios: $f\tau_M$ and $f\tau_R$.
- E maximizes in a certain parameter domain for the two time ratios.
- The black line shows the path as frequency varies for the given co-axial injector, chamber conditions, and propellants.

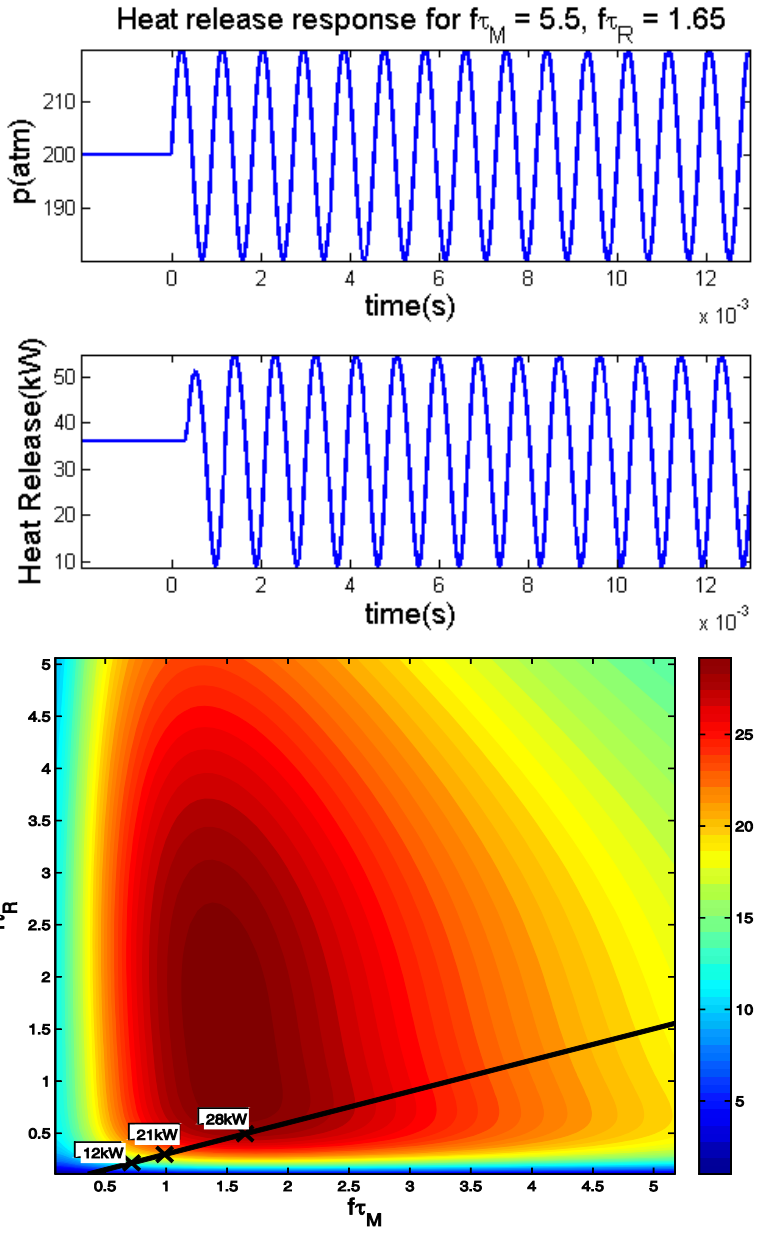

Long-time Pressure Amplitude vs. Triggering Disturbance Amplitude

-- At this operating point, there is a stable steady-state, an unstable limit-cycle, and a stable limit cycle.

-- Small disturbances decay with time.

-- Above a threshold amplitude but below the steady limit-cycle amplitude, growth to the limit cycle occurs.

-- The threshold is the unstable limit-cycle amplitude.

-- Disturbances with amplitude larger than the stable limit cycle value will decay to the limit cycle.

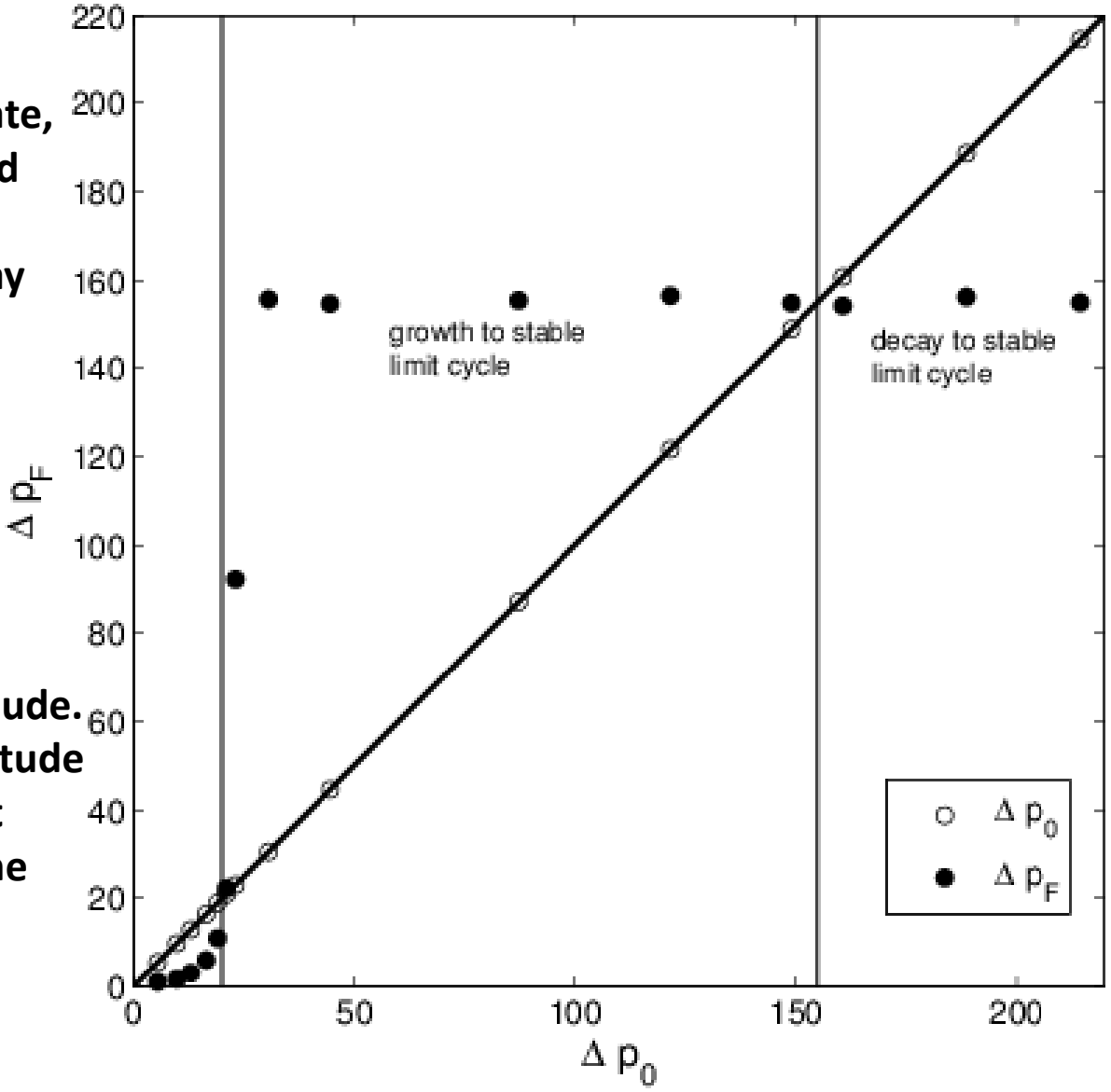

Wave Profiles

For these cases, the initial disturbance had the form of a solution to the linear wave equation for some tangential mode (e. g., first tangential, second tangential , or first radial). So, a Bessel function described radial behavior while a trigonmetric function described azimuthal behavior.

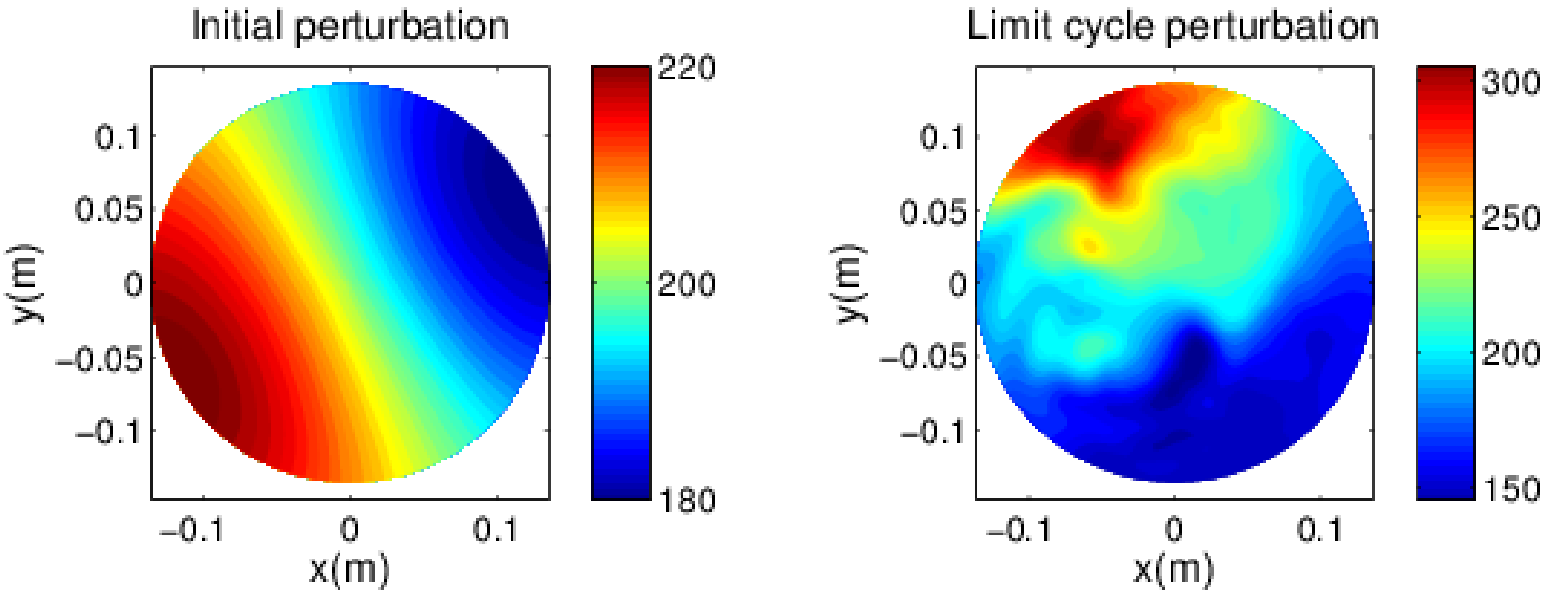

The nonlinear resonance introduces other modes, harmonics and sometimes sub-harmonics. For tangential modes, frequencies are not integer multiples of lower mode frequency. So, the limit cycle need not be perfectly periodic. It is usually characterized by the frequency of the largest Fourier component.

LIMIT-CYCLE DESCRIPTIONS – PHASE PLANE

(left) Disturbance amplitude larger than stable limit-cycle amplitude: decay to limit-cycle.

(right) Disturbance amplitude less than stable limit-cycle amplitude: growth to stable limit-cycle.

(bottom) Disturbance amplitude less than unstable limit-cycle amplitude: decay to steady-state.

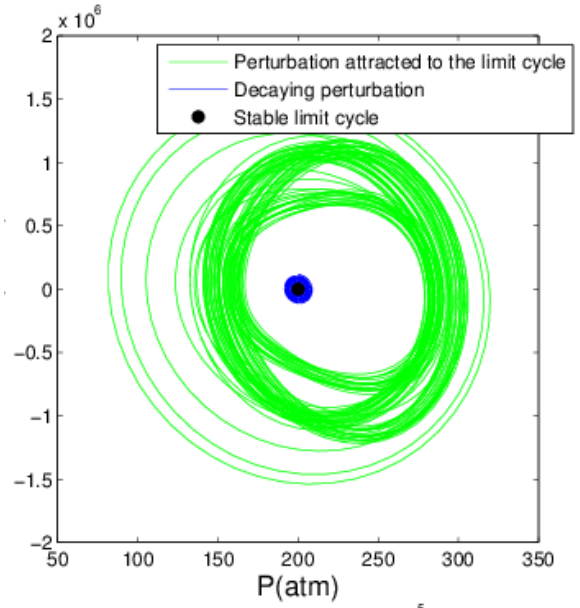

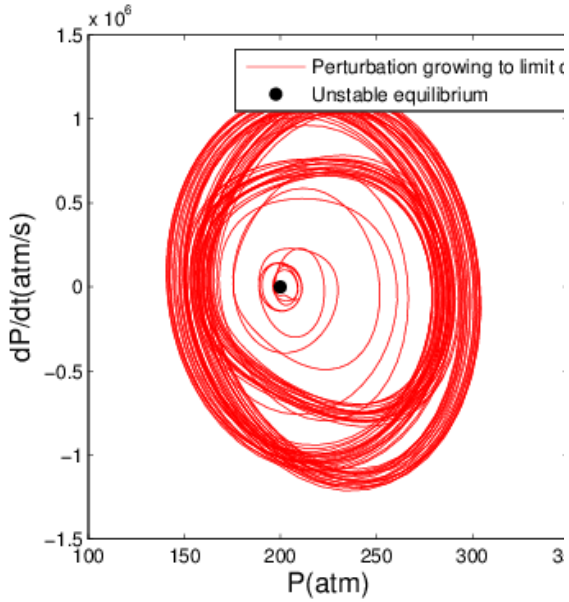

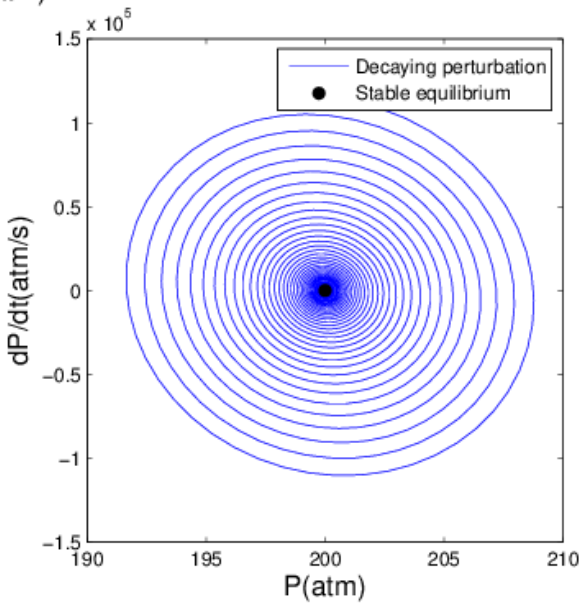

Ten-injector Simulation

An initial condition of a 1T mode with sufficient amplitude results in triggering. Below a threshold for initial amplitude, decay and stability result. Above the threshold, a stable limit cycle develops.

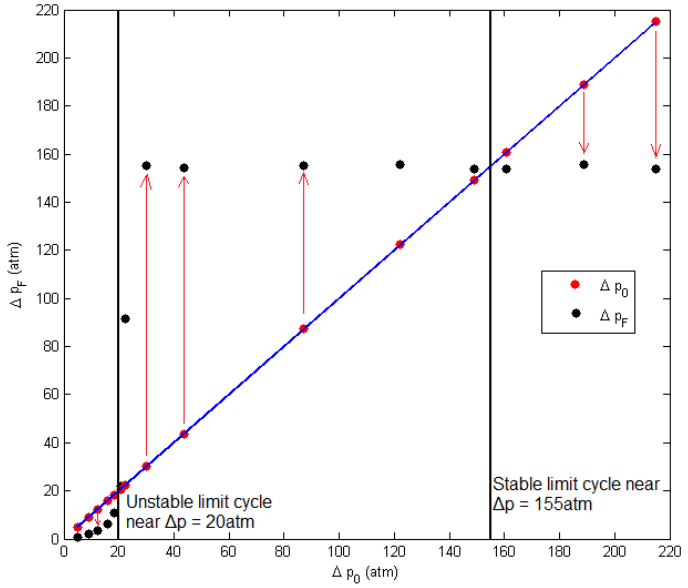

The frequency spectrum analysis shows that nonlinear resonance, in this case, produces a 1T mode, a 2T mode , and a sub-harmonic with frequency equal to difference of 1T and 2T frequencies.

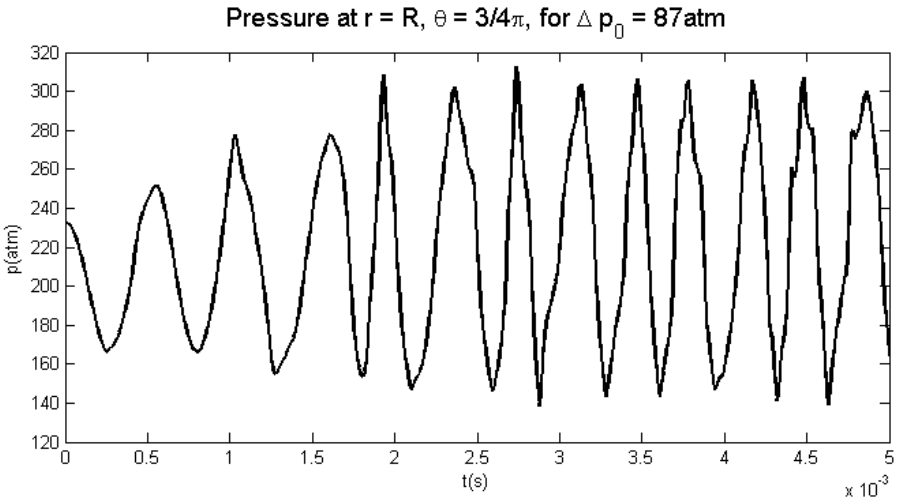

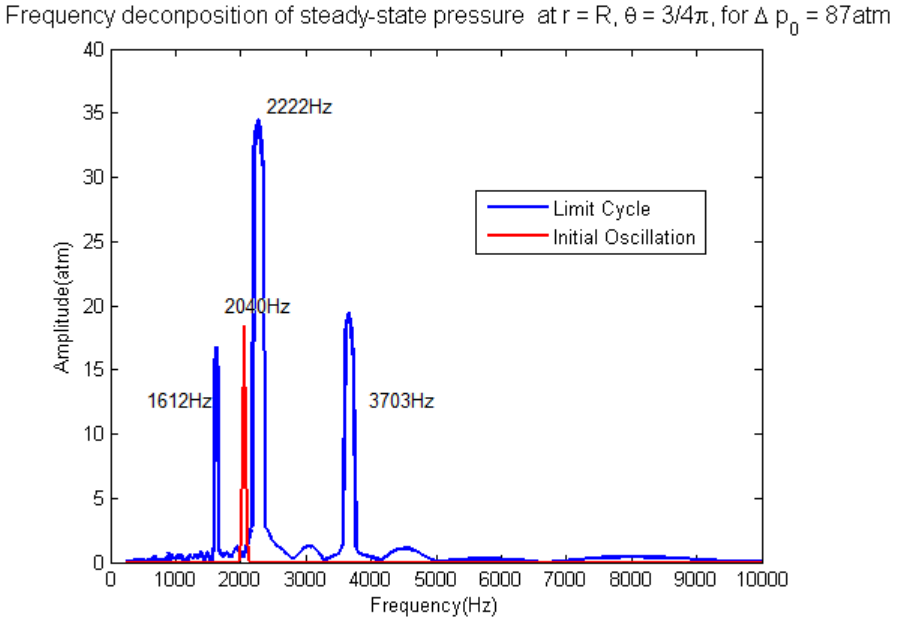

Sub-harmonics and Nearly Periodic Limit Cycles

-- A sub-harmonic mode often appears in nonlinear resonance with a frequency equal to the sum or difference of integer multiples of natural frequencies.

-- The presence of the 1T, 2T, and sub-harmonic modes prevents a periodic behavior. If one natural mode dominates, a nearly periodic behavior results.

-- Linear theory does not predict the existence of harmonics for circular cylinders or sub-harmonics for any chamber.

-- Galerkin methods require the assumption of the modes present; they do not predict the presence independently.

Left: disturbance decays

Right: growth occurs with new modes and aperiodic behavior

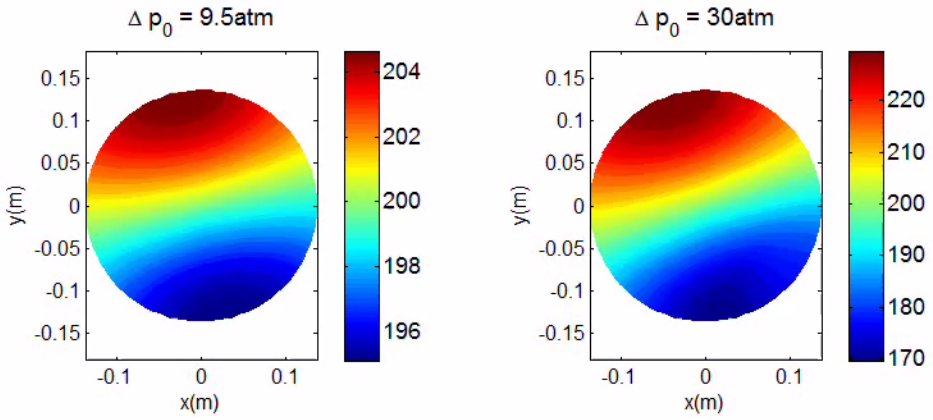

Pure Second Tangential (2T) Mode is the Initial Condition

Triggering is possible.
Nonlinear resonance induces fourth tangential mode plus first harmonic of 2T.
No 1T or sub-harmonic.

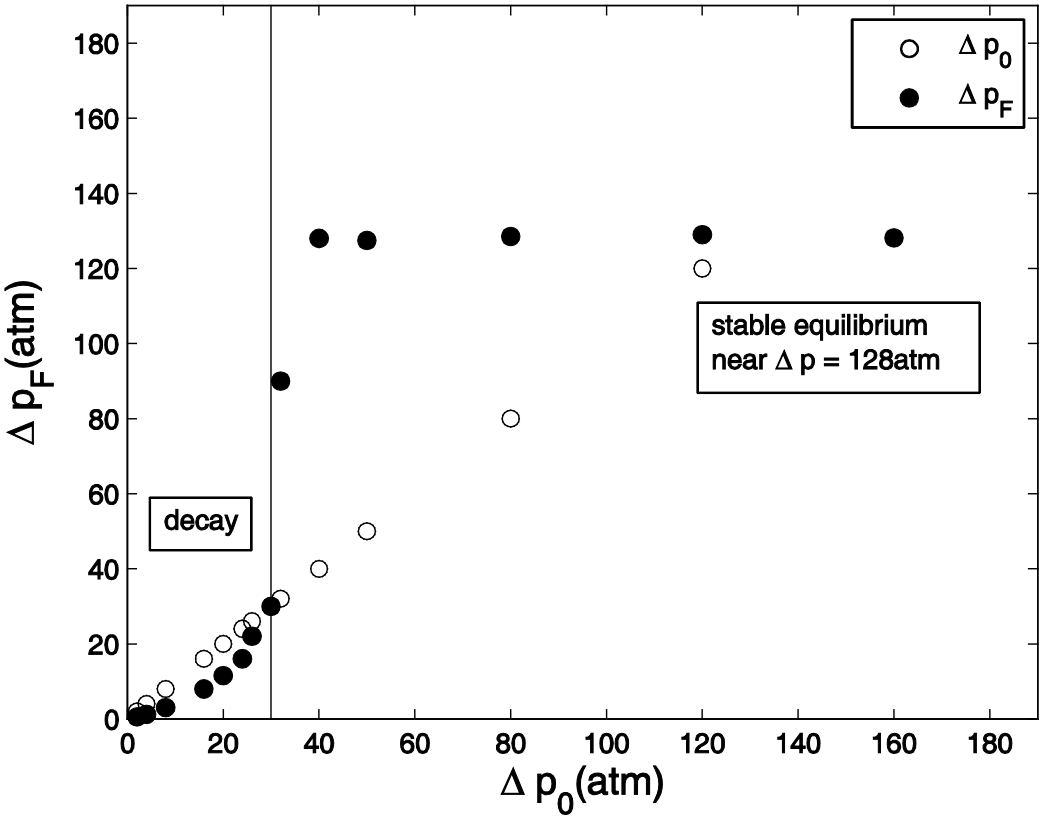

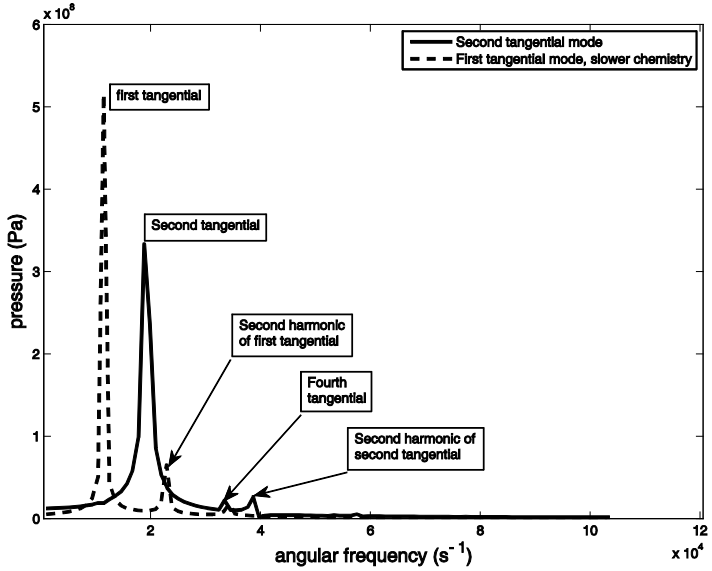

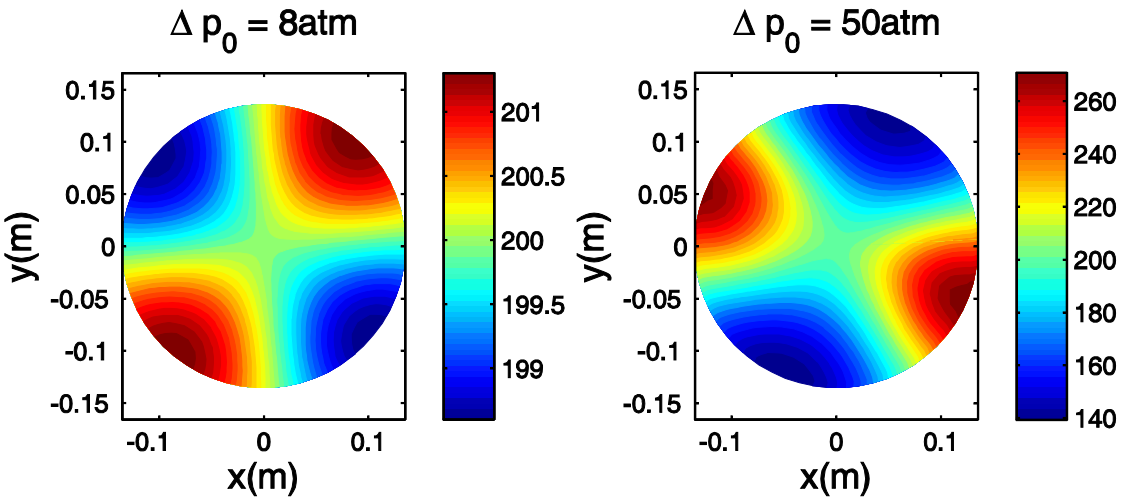

Comparison of Variations in E and p

-- E is found to lag p in time t and position θ for tangential spinning modes. Example with 2T mode below.

-- Energy release is localized in the ten injector streams but differences from one stream to another occur due to pressure phasing.

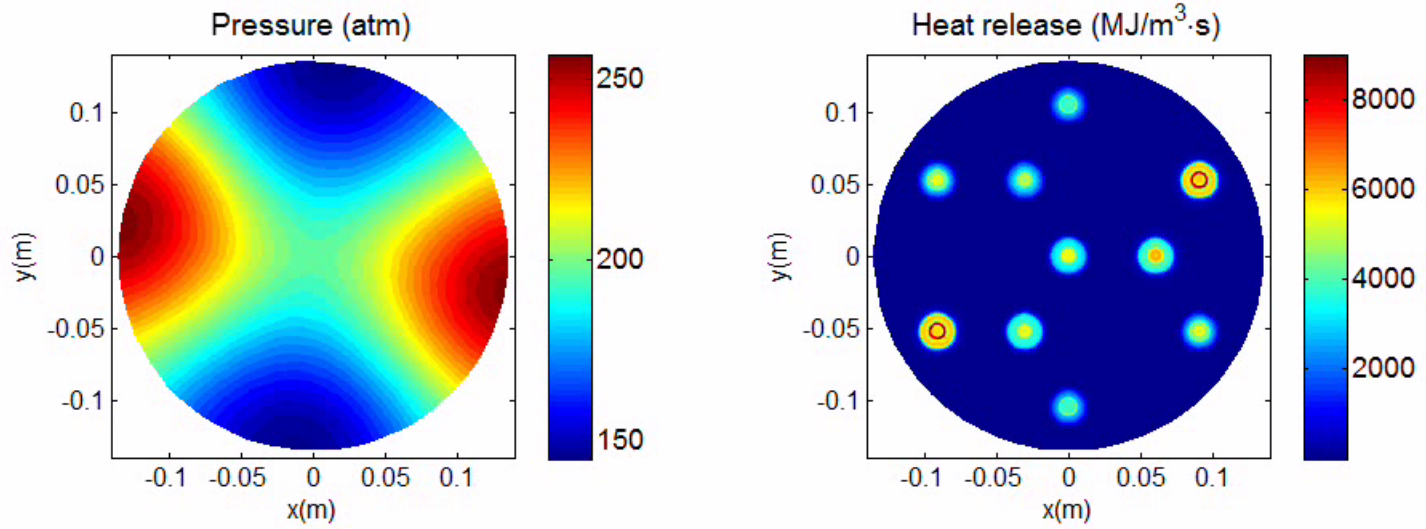

Test with Variation in Reaction Time

-- 1T mode is initial condition.
-- Chemical kinetic constant is changed causing longer reaction time.
-- The black line in contour plot adjusts and 2T position moves to a less sensitive region.
-- Consequently, nonlinear resonance does not include 2T and sub-harmonic.
-- Nonlinear resonance now involves energy transfer to harmonics of 1T mode.

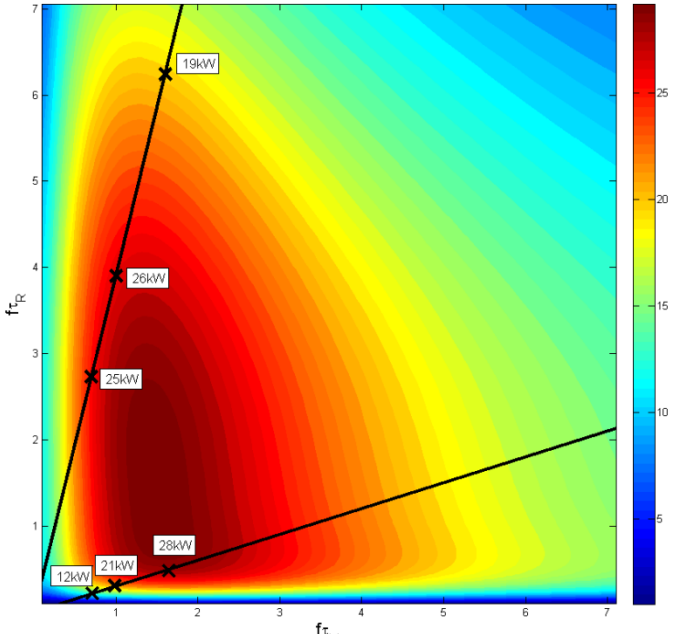

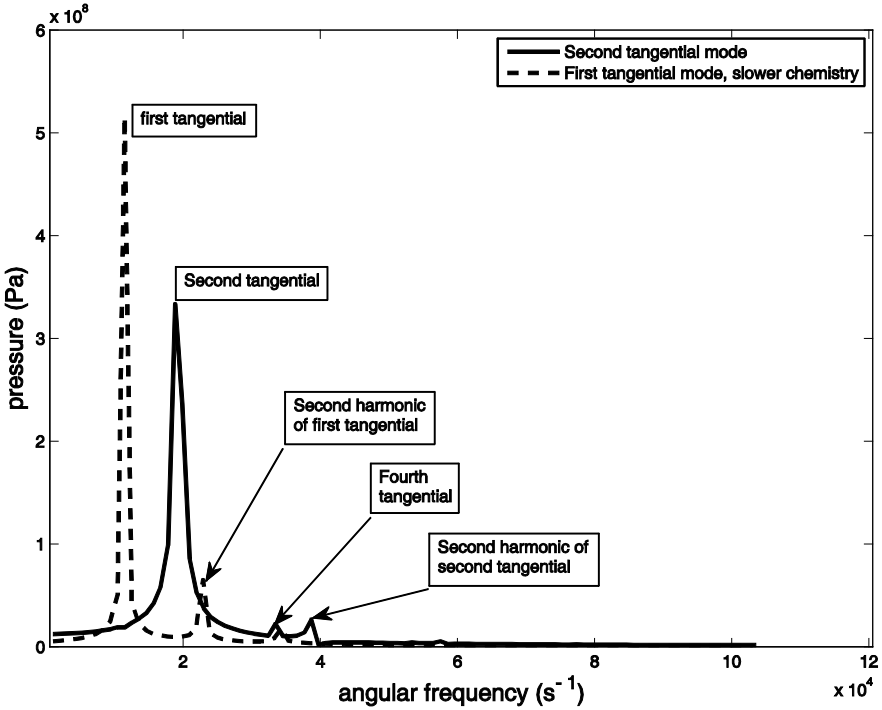

Energy of Threshold Pulse

Over a wide range, threshold triggering pressure amplitude is approximately inversely proportional to Gaussian pulse width. Since acoustical energy is proportional to the integral of the pressure squared over the 2D domain, there is a constant threshold energy.

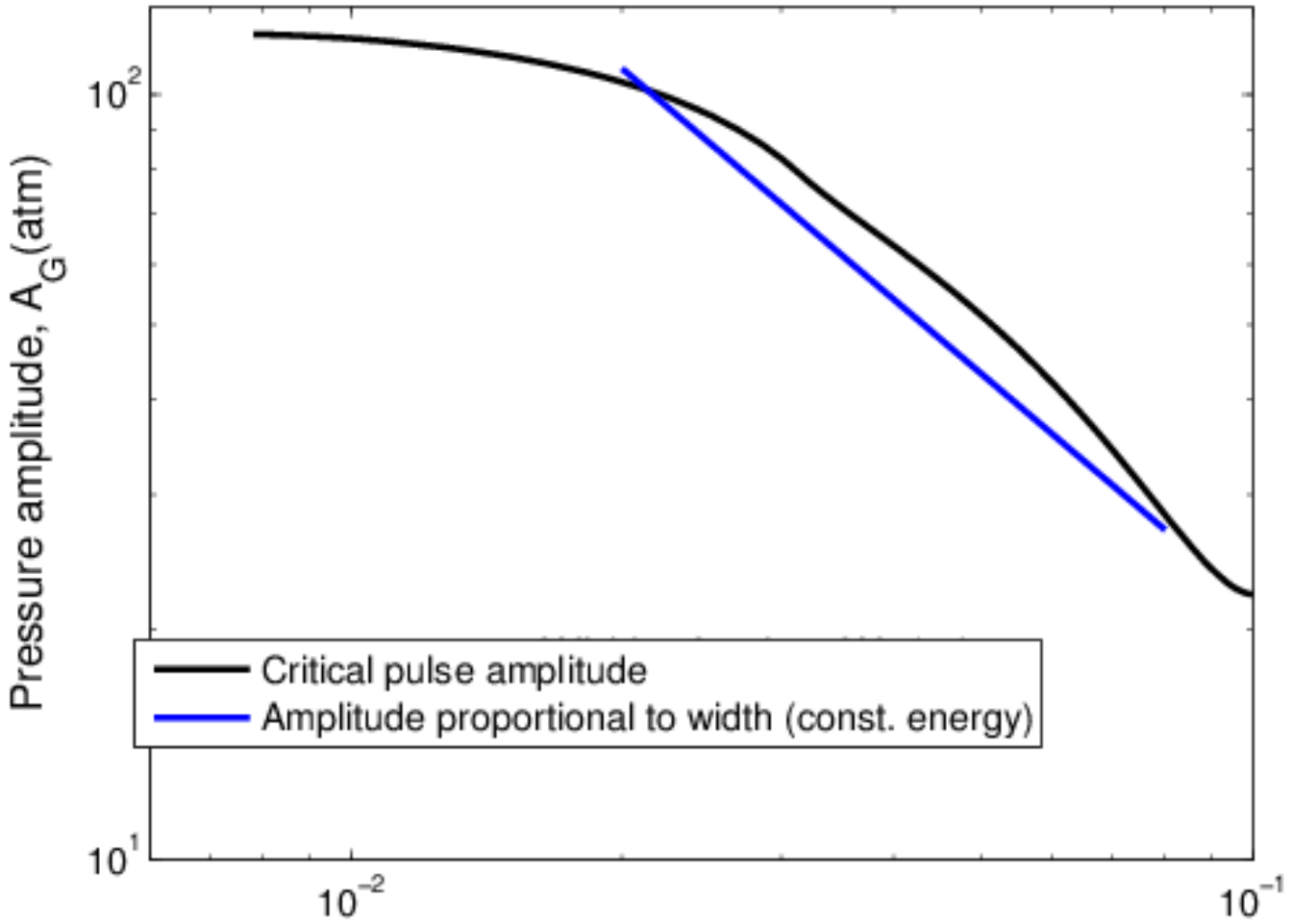

Conclusions from model-equation solution with co-axial injection, mixing and reaction

- **A nonlinear acoustics model for transverse modes and a co-axial model for propellant mixing and reaction are used to study combustion dynamics with a ten-injector geometry.**
- **Triggering of 1T and 2T are possible; both stable and unstable limit cycles are identified. The stable limit behavior is not always exactly periodic.**
- **Two characteristic combustion times are found and prove to be critical. Accordingly, a time-lag in the combustion response is found.**
- **Depending on characteristic time and frequency values, nonlinear resonance can transfer energy to second tangential mode (2T) and to a sub-harmonic mode. Or energy can be transferred to higher harmonics. The instability occurs for a frequency where the heat-release response to pressure variation is very strong.**
- **Triggering can result from either disturbances with well defined profiles corresponding to natural modes or localized disturbances.**
- **Directional travel orientation of a local disturbance is consequential for triggering. Different stability and different limit cycles can be induced.**
- **Approximately, a constant energy threshold for triggering is seen.**

Stochastic Analysis of Triggering Mechanism:

Polynomial Chaos Expansion (PCE) Method

The several characteristics of the disturbing pulse will be the random variables (RV) and form the vector ξ.

-- Equations for wave dynamics governing pressure and velocity.

$$\mathcal{L}_1\left(\mathbf{n}, r, \theta, t, \boldsymbol{\xi}\right) = \mathbf{f}_1\left(r, \theta, t, \mathbf{m}, \boldsymbol{\xi}\right)$$

-- Diffusion/advection/reaction equations for each injector governing temperature and mass fractions.

$$\mathcal{L}_2\left(\mathbf{m}, x, \eta, t, \boldsymbol{\xi}\right) = \mathbf{f}_2\left(x, \eta, t, \mathbf{n}, \boldsymbol{\xi}\right)$$

-- Expand the dependent variables in a series of Legendre polynomials (PCE)

$$\mathbf{n}\left(r, \theta, t, \boldsymbol{\xi}\right) \approx \sum_{k=0}^{P} \mathbf{n}_k\left(r, \theta, t\right) \Psi_k\left(\boldsymbol{\xi}\right)$$

$$\mathbf{m}\left(x, \eta, t, \boldsymbol{\xi}\right) \approx \sum_{k=0}^{P} \mathbf{m}_k\left(x, \eta, t\right) \Psi_k\left(\boldsymbol{\xi}\right)$$

-- Truncate to "converge" the series.

***P+1 = (n+ l)! /(n! l!), l* is degree of polynomial, *n* is number of RV.**

-- Substitute PCE in equations and solve resulting PDEs for coefficients by finite-differences.

$$\left\langle \mathcal{L}_1\left(r, \theta, t, \boldsymbol{\xi}; \sum_{k=0}^{P} \mathbf{n}_k\left(r, \theta, t\right) \Psi_k\left(\boldsymbol{\xi}\right)\right) \middle| \Psi_i\left(\boldsymbol{\xi}\right) \right\rangle = \left\langle \mathbf{f}_1\left(r, \theta, t, \mathbf{m}, \boldsymbol{\xi}\right) \middle| \Psi_i\left(\boldsymbol{\xi}\right) \right\rangle$$

$$\left\langle \mathcal{L}_2\left(x, \eta, t, \boldsymbol{\xi}; \sum_{k=0}^{P} \mathbf{m}_k\left(x, \eta, t\right) \Psi_k\left(\boldsymbol{\xi}\right)\right) \middle| \Psi_i\left(\boldsymbol{\xi}\right) \right\rangle = \left\langle \mathbf{f}_2\left(x, \eta, t, \mathbf{n}, \boldsymbol{\xi}\right) \middle| \Psi_i\left(\boldsymbol{\xi}\right) \right\rangle$$

Prediction of Probability of Triggering

- **For each set of RV values describing a disturbance, i.e., value of the vector ξ , the outcome is a random variable with value of unity or zero; if a limit-cycle is triggered, the outcome is given value one while if decay of amplitude occurs, a value of zero is given.**
- **Each value of ξ gives a distinct realization for the values of the field variables, e.g., pressure, velocity, temperature, and mass fractions.**
- **Every realization has the same values for the coefficients in the PCE series.**
- **Two types of pulsed disturbances were examined: (i) repeated Gaussian pulse and (ii) oscillating dipole pulse. Both have orientations.**
- **A marginal triggering probability is obtained, as a function of one of the *n* random variables (RV), with value between one and zero by integrating over the other *n-1* variables.**
- **The outcome is predicted by PCE calculations of each realization over twelve oscillation periods. The accuracy is evaluated by comparison to selected realizations using 120 periods.**
- **The accuracy of the PCE calculations of the field variables can be evaluated by comparison with direct solution of the original PDEs.**
- **PCE computational efficiency is compared to the results of Monte Carlo calculations.**

Calculations with PCE. Normally, 12 oscillation cycles are sufficient to predict outcome.
Near unstable limit-cycle, slow growth behavior was checked with 120 cycles.
PCE calculations compare favorably with direct solution of original PDEs.

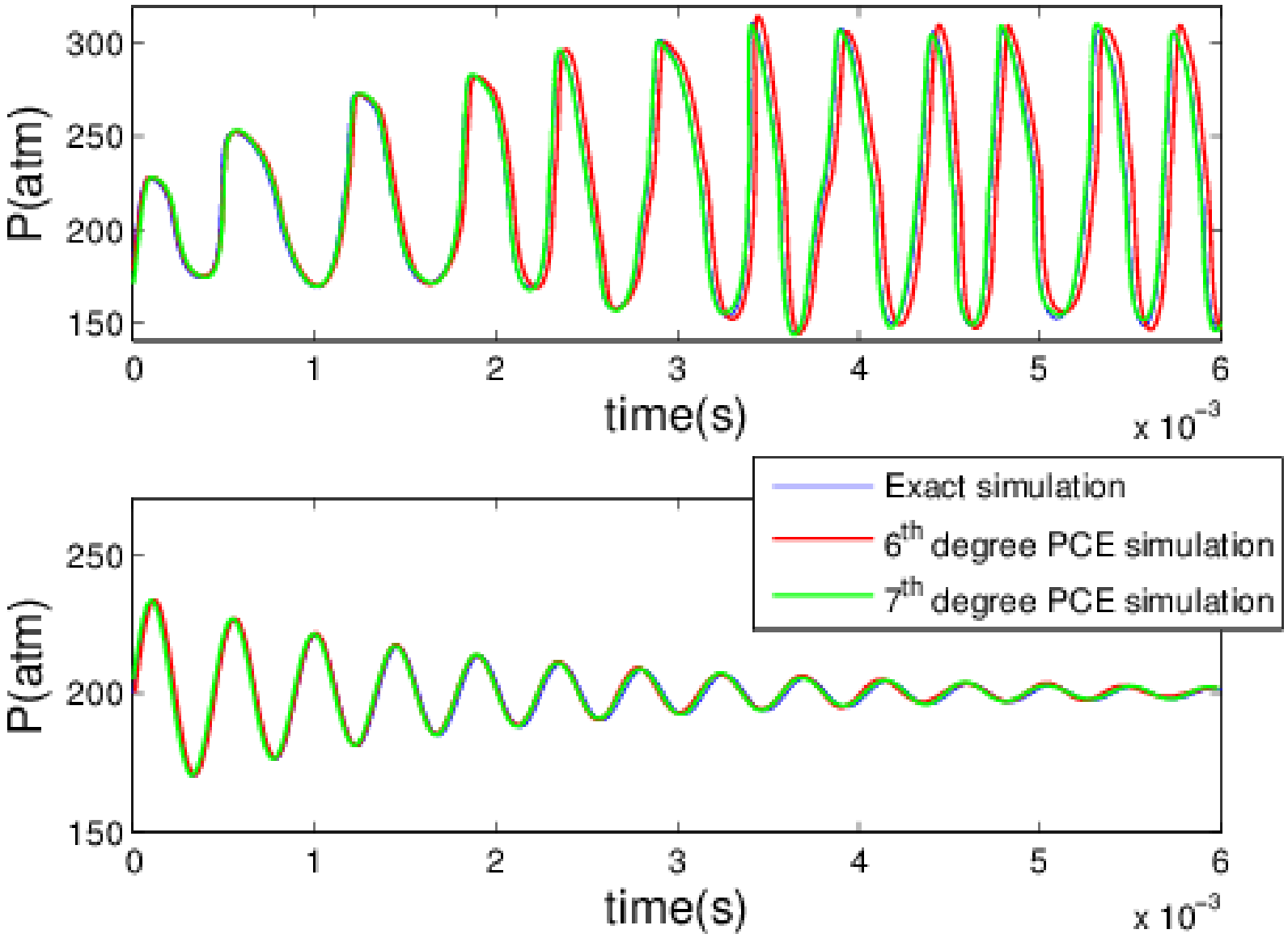

The PCE accuracy with 7th degree polynomial is quite satisfactory.

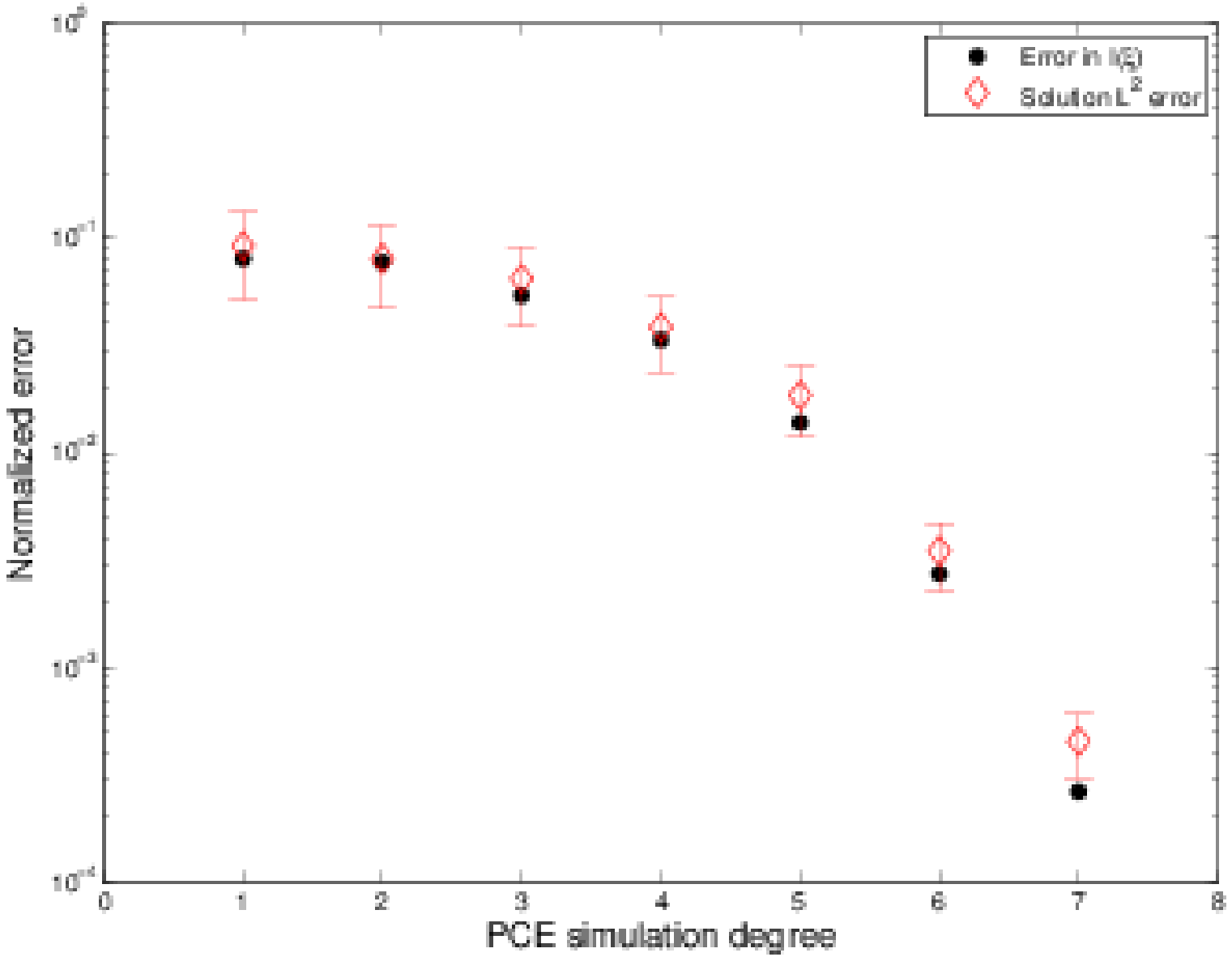

A marginal probability is determined by integrating results over *n-1* random variables. Comparisons are made with 95% confidence intervals Monte Carlo (MC) simulations using direct solutions of original PDEs. Dipole disturbance gives expected results where probability of triggering increases with pulse magnitude.

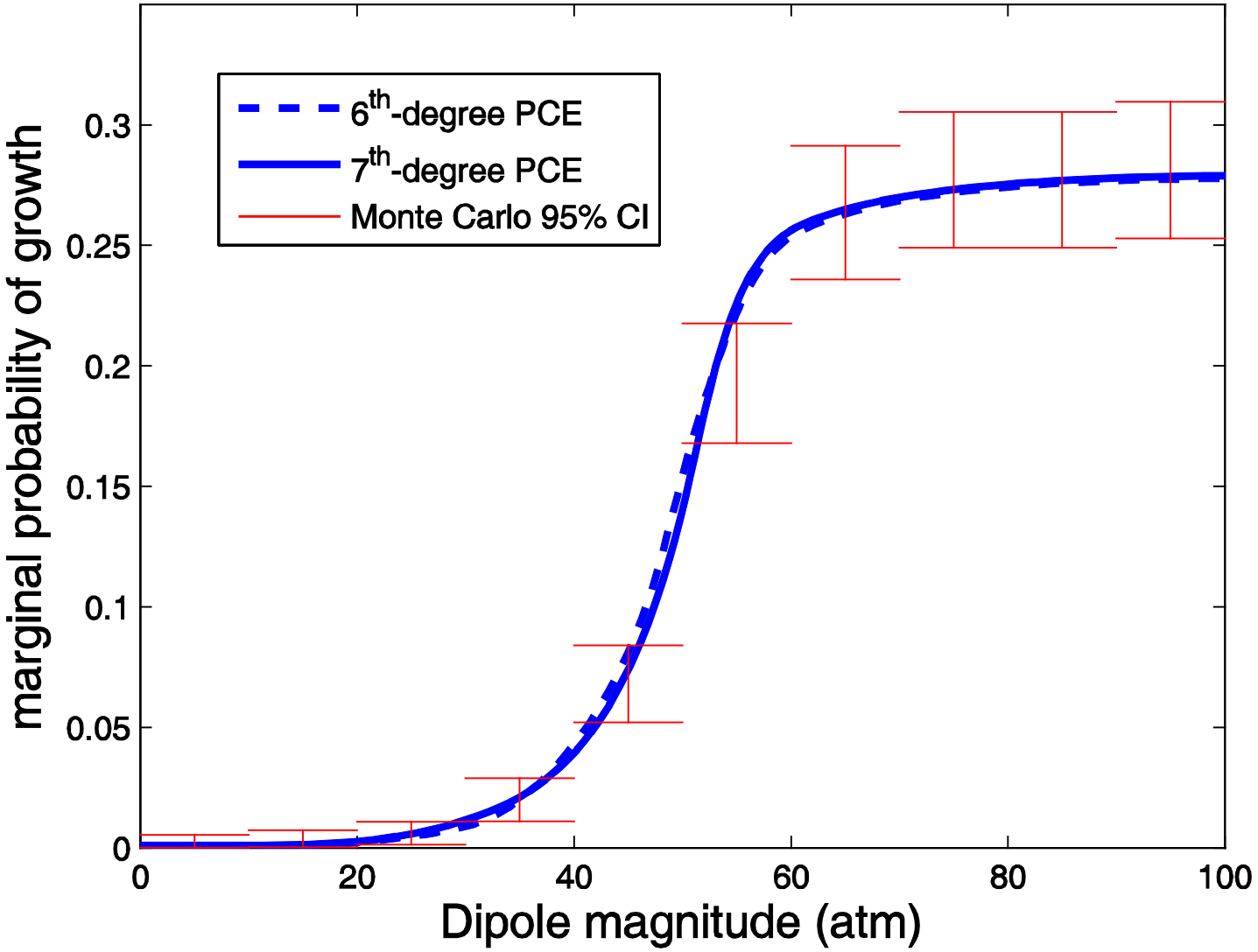

Triggering is most probable when dipole period is close to natural chamber period.

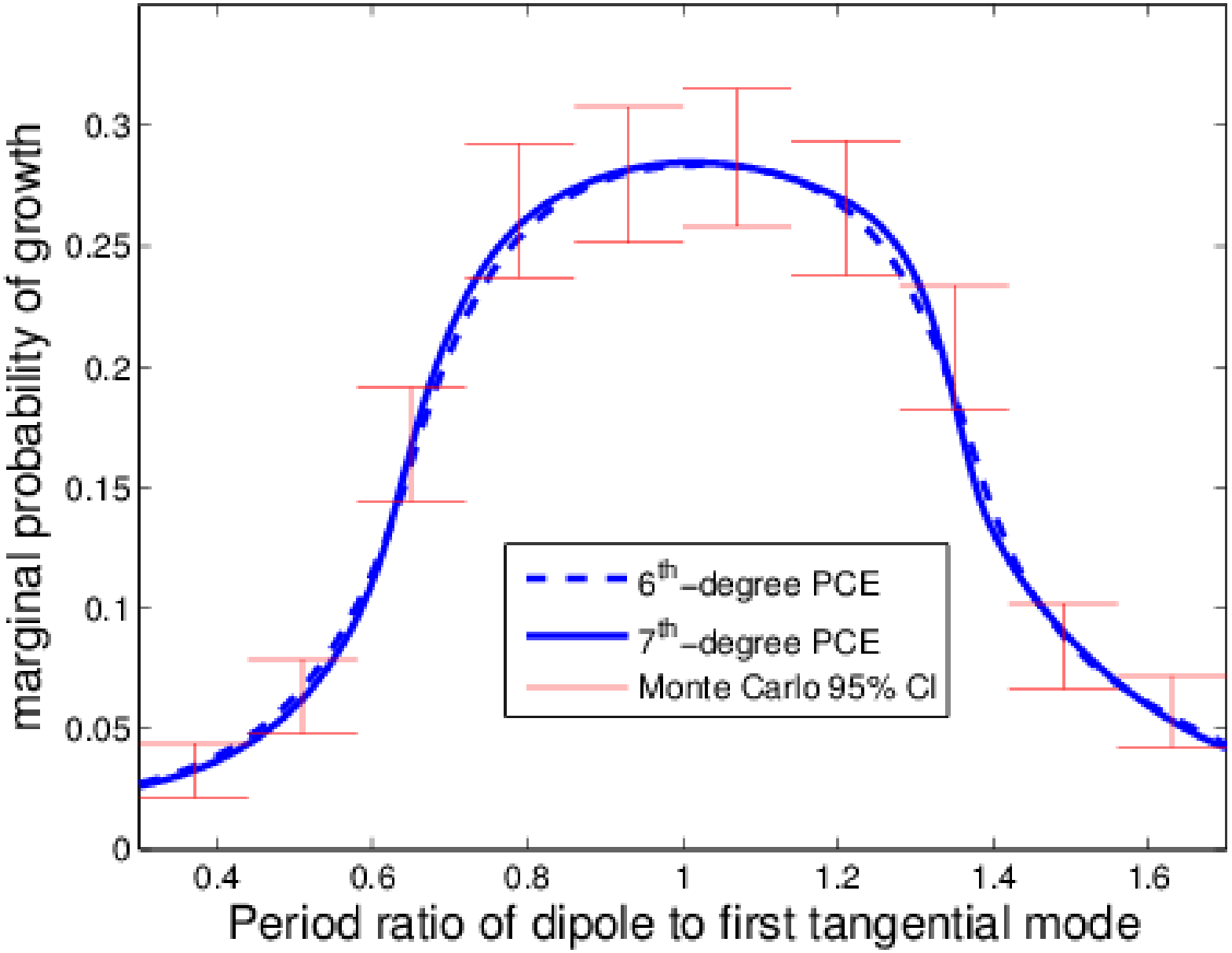

For triggering of spinning (standing) wave, orientation is wanted (not wanted) and pulsing duration matching an odd (any) multiple of chamber half (full) period is optimal.

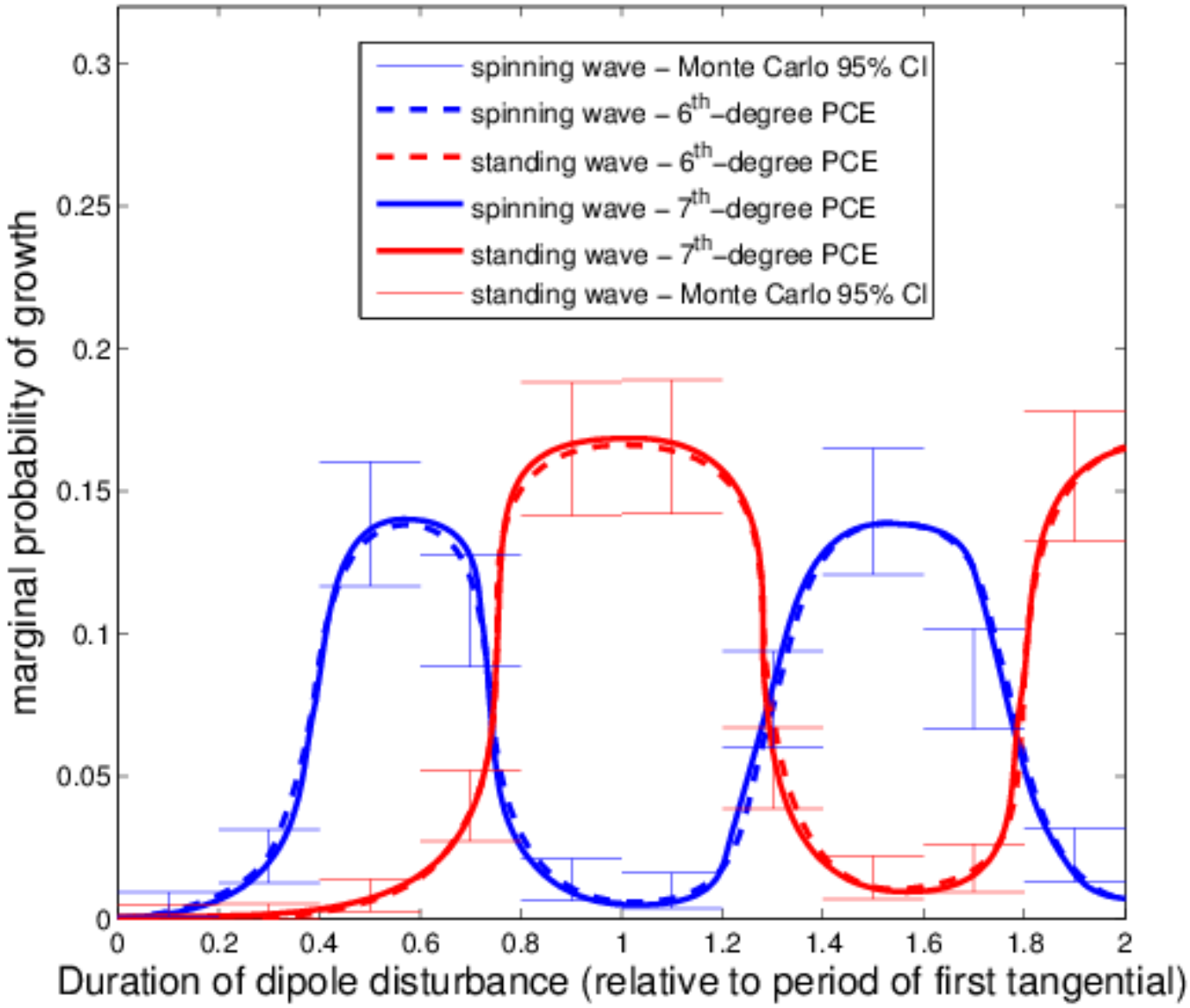

Triggering of first tangential mode is most probable when pulse is centered near the outer wall .

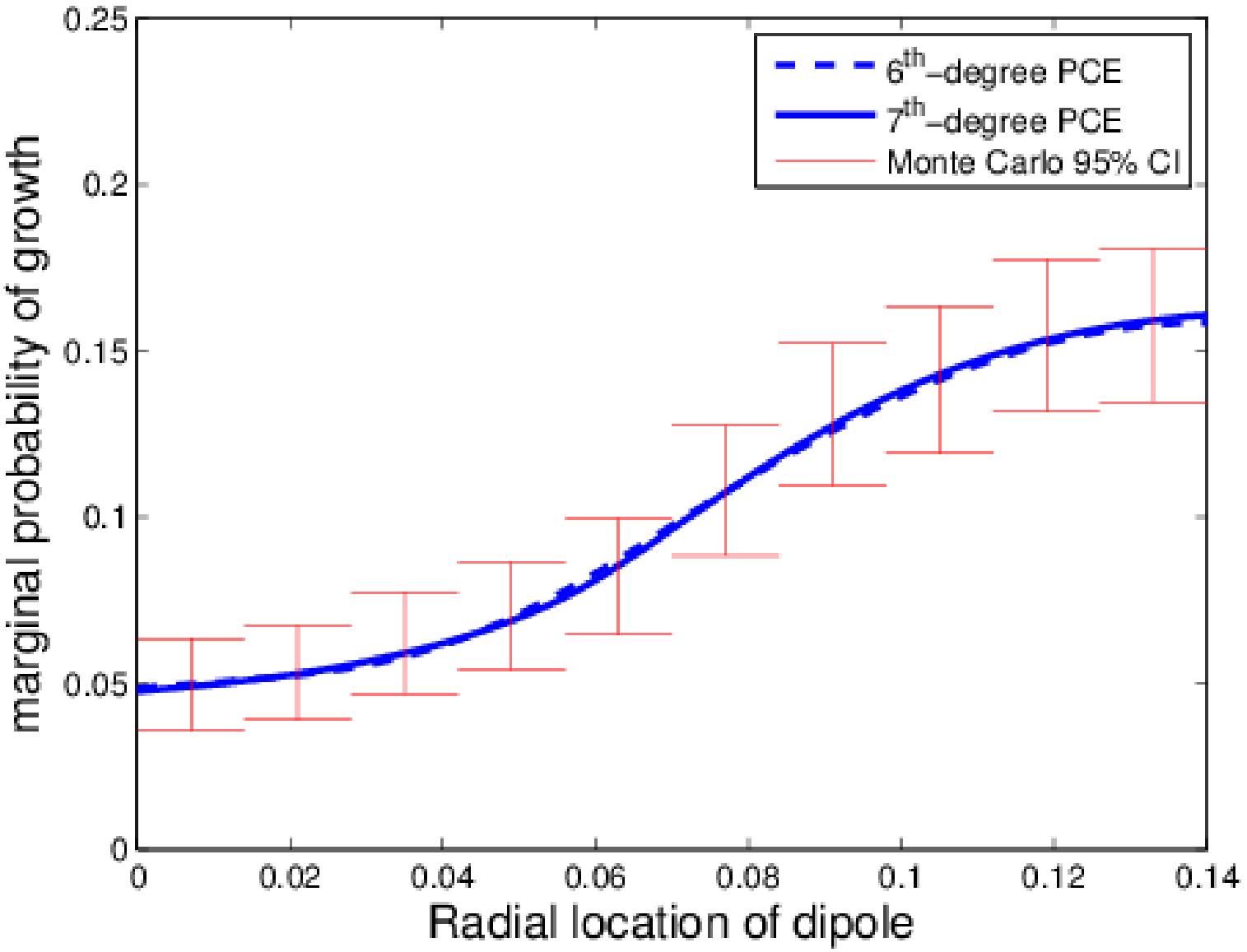

Tangential orientation of dipole is optimal for triggering first tangential mode oscillation.

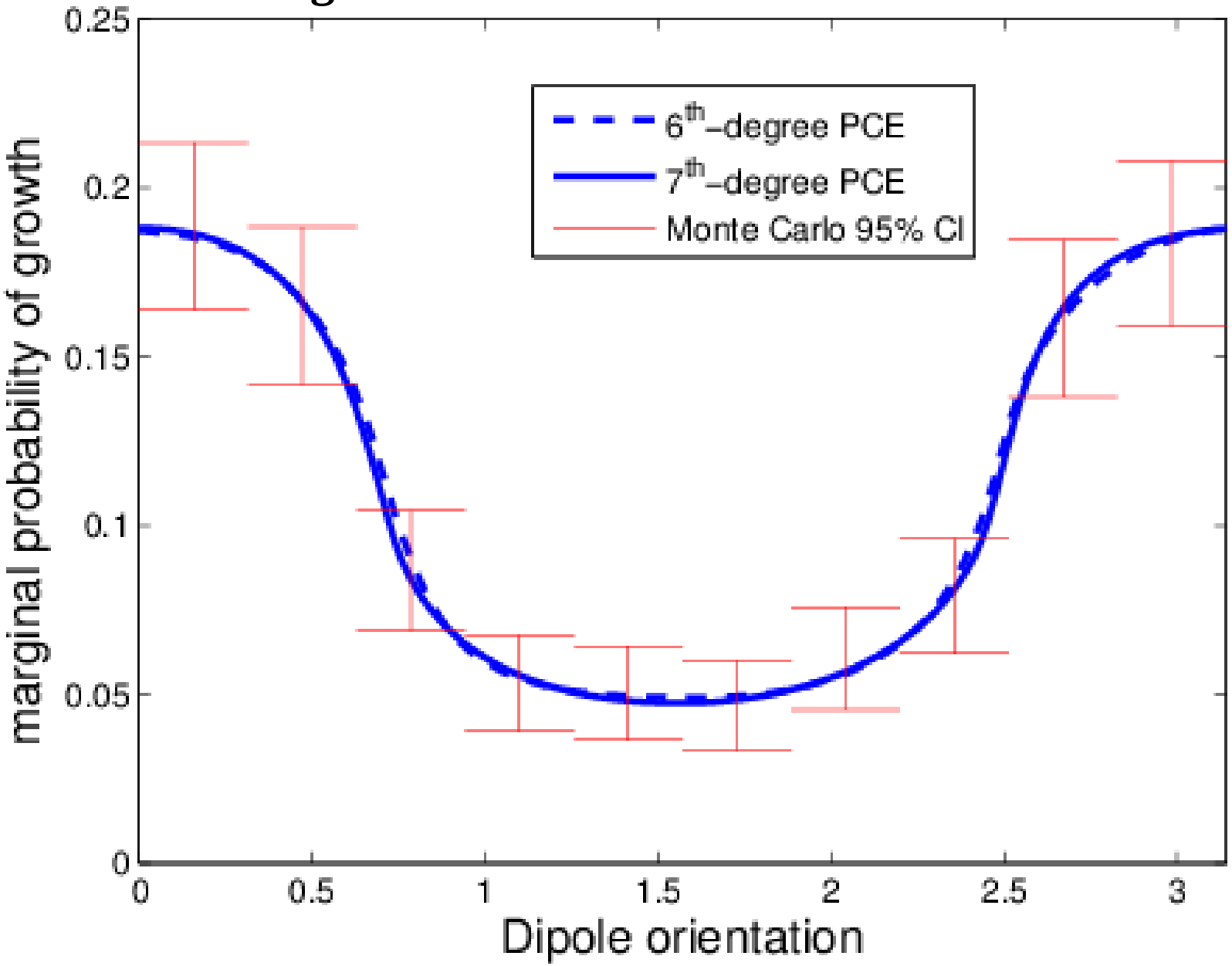

Joint probability displays can be informative. For example, The maxima and minima of previous plots lead to a saddle-shaped behavior for the probable outcome with magnitude and orientation variations.

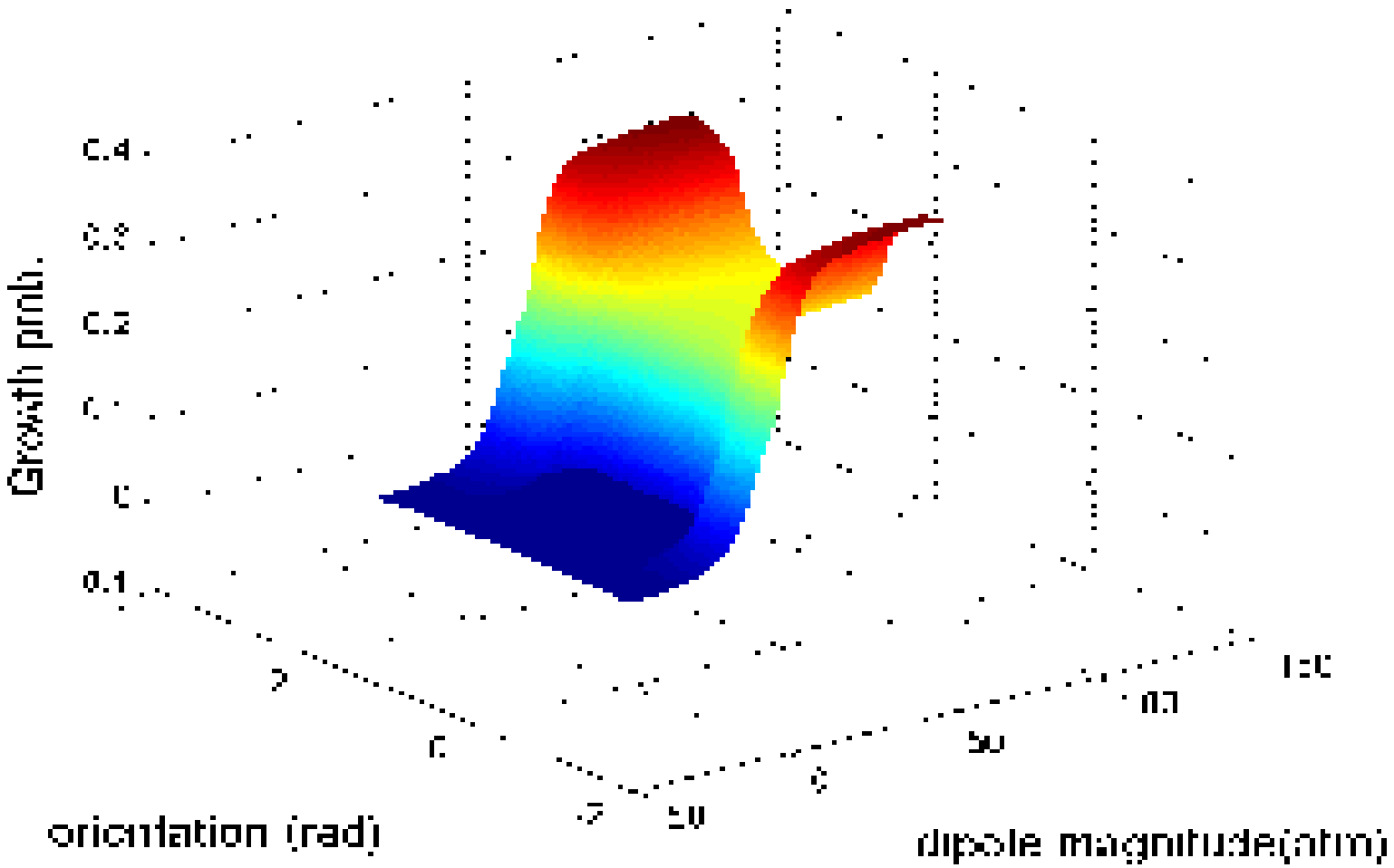

Second-order accuracy in finite-difference calculations for PCE coefficients yields second-order accuracy in probability calculations.

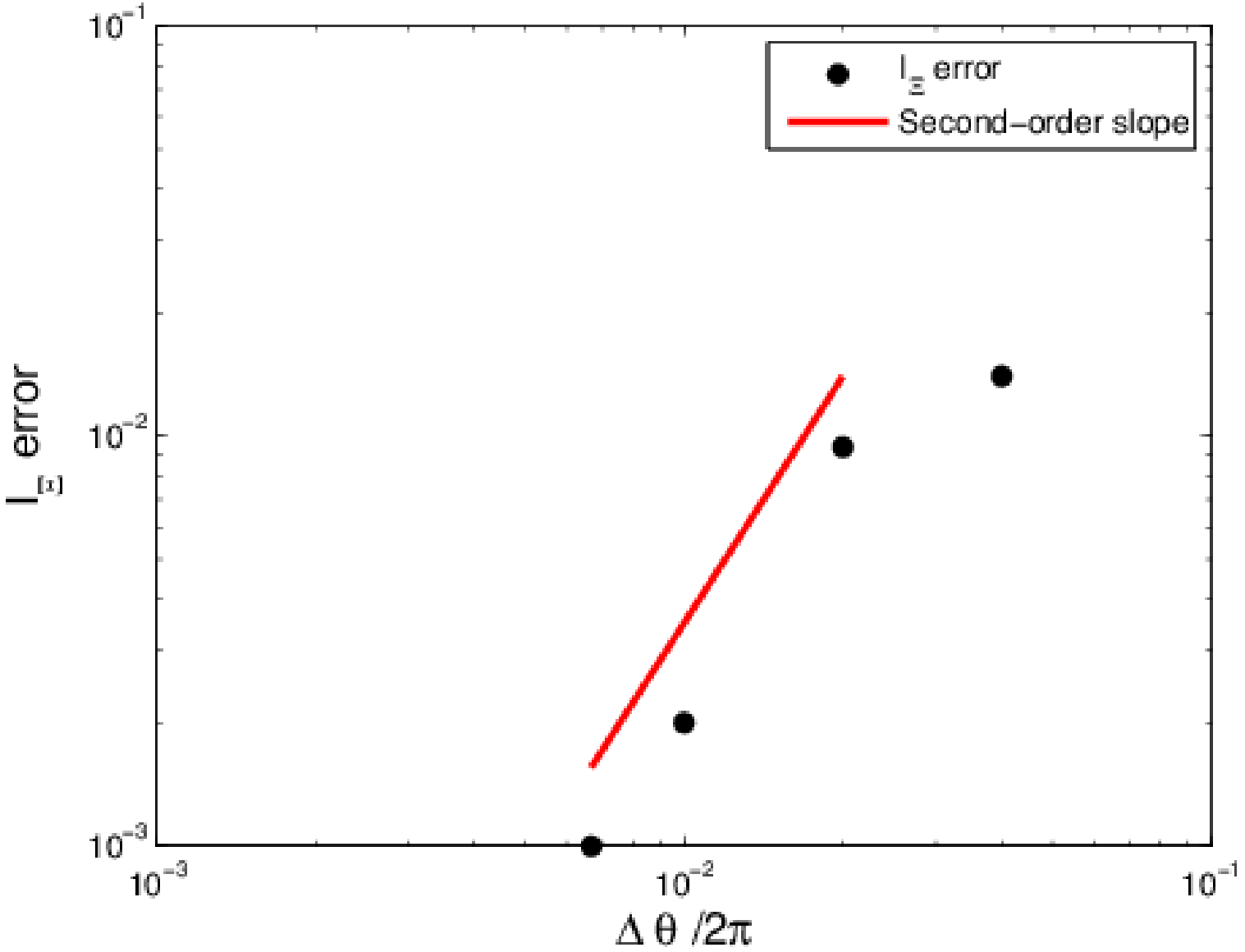

For the limited number of RV here and the desired accuracy, the PCE calculations are substantially less costly than MC.

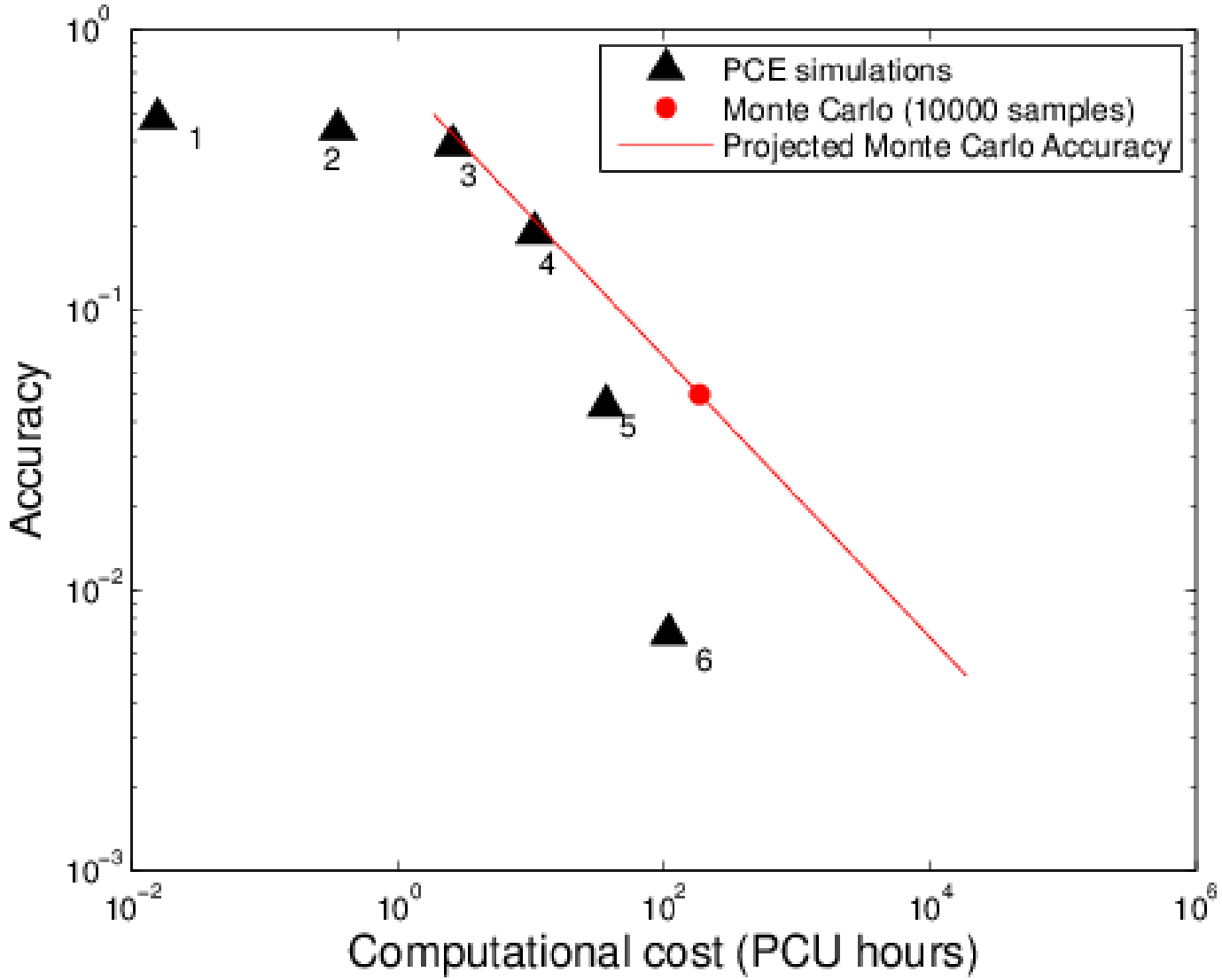

CONCLUSIONS

-- Probability of Triggering may be calculated by PCE or MC methods.
-- For the RV number here, PCE is substantially more efficient than MC.

ONGOING STUDIES

-- Relate pulse disturbances to physical causes, e.g., upstream flow in propellant feed systems.
-- Model longitudinal mode oscillations.

FUTURE STUDIES

-- Develop control strategies to arrest triggering action.

Thank you.